crystals

MDPI

Article

High Current Density Trench CAVET on Bulk GaN Substrates with Low-Temperature GaN Suppressing Mg Diffusion

Xinyi Wen [1], Kwang Jae Lee [1], Yusuke Nakazato [1,2], Jaeyi Chun [1] and Srabanti Chowdhury [1,*]

[1] Department of Electrical Engineering, Stanford University, Stanford, CA 94305, USA; xinyiwen@stanford.edu (X.W.)
[2] Kyocera Corporation, 45 Wadai, Tsukuba, Ibaraki 300-4247, Japan
* Correspondence: srabanti@stanford.edu

Abstract: We report that, for the first time, a low-temperature GaN (LT-GaN) layer prepared by metal–organic chemical vapor deposition (MOCVD) regrowth was used as a Mg stopping layer (MSL) for a GaN trench current–aperture vertical electron transistor (CAVET) with p-GaN as a carrier blocking layer (CBL). Inserting LT-GaN on top of the p-GaN effectively suppresses Mg out-diffusion into the regrown AlGaN/GaN channel, contributing to the high current capability of GaN vertical devices with a p-GaN CBL. With different MOCVD growth conditions, MSLs inserted in trench CAVETs were comprehensively investigated for the influence of MSL regrowth temperature and thickness on device performance. With the best on-state current performance obtained in this study, the trench CAVET with a 100 nm thick MSL regrown at 750 °C shows a high drain current of 3.2 kA/cm^2 and a low on-state resistance of 1.2 mΩ·cm^2. The secondary ion mass spectrometry (SIMS) depth profiles show that the trench CAVET with the 100 nm thick MSL regrown at 750 °C has a dramatically decreased Mg diffusion decay rate (~39 nm/decade) in AlGaN/GaN channel, compared to that of the CAVET without a MSL (~104 nm/decade). In developing GaN vertical devices embedded with a Mg-doped p-type layer, the LT-GaN as the MSL demonstrates a promising approach to effectively isolate Mg from the subsequently grown layers.

Keywords: gallium nitride (GaN); current aperture vertical electron transistor (CAVET); trench CAVET; GaN vertical transistor; Mg memory effect; diffusion; MOCVD

Citation: Wen, X.; Lee, K.J.; Nakazato, Y.; Chun, J.; Chowdhury, S. High Current Density Trench CAVET on Bulk GaN Substrates with Low-Temperature GaN Suppressing Mg Diffusion. *Crystals* **2023**, *13*, 709. https://doi.org/10.3390/cryst13040709

Academic Editor: Evgeniy N. Mokhov

Received: 28 March 2023
Revised: 12 April 2023
Accepted: 14 April 2023
Published: 21 April 2023

Copyright: © 2023 by the authors. Licensee MDPI, Basel, Switzerland. This article is an open access article distributed under the terms and conditions of the Creative Commons Attribution (CC BY) license (https://creativecommons.org/licenses/by/4.0/).

1. Introduction

Over the last two decades, gallium nitride (GaN) has emerged as a strong candidate to develop electronic devices in high-power fast-switching applications due to its superior material properties such as high critical field, high saturation velocity, and high thermal conductivity [1]. In general, GaN-based power transistors are fabricated either in lateral-type devices using foreign substrates such as Si, SiC, and sapphire, or in vertical-type devices grown on a homogeneous GaN substrate [2]. Compared to the typical lateral GaN device high electron mobility transistor (HEMT), vertical power device topologies allow higher off-state blocking capability since the breakdown voltage scales with the drift layer thickness while maintaining a more uniform electric field distribution [3–5].

To date, various three-terminal GaN vertical devices have been successfully developed, such as metal oxide semiconductor field effect transistors (MOSFETs) [6], static induction transistors (SITs) [7], and current aperture vertical electron transistors (CAVETs) [8–10]. Among the various vertical power transistors, CAVET is unique in its merging of a lateral 2DEG channel with a vertical drift region. A CAVET device, therefore, efficiently takes the benefit of high current density and high breakdown voltage inherent to the vertical structure while combining the advantage of the high conductivity of polarization-induced 2DEG at the AlGaN/GaN interface in HEMTs [11]. This feature of CAVETs makes it especially attractive to offer high current density in vertical devices.

The formation of p-type GaN films is a key technology in developing vertical power devices, and magnesium (Mg) is a commonly-used acceptor dopant in GaN. Among the reported CAVET studies, many of them inserted a p-GaN layer as the carrier blocking layer (CBL) with Mg doping either by metal-organic chemical vapor deposition (MOCVD) or by ion-implantation, to form a p-n body junction in the bulk for sustaining the blocking field in the off-state. However, there is a widely observed problem with the Mg-doped p-GaN layer sandwiched between the n-type or unintentionally doped (UID) GaN layers called the "memory effect", whereby Mg inevitably out-diffuses into adjacent regions during the growth process at high temperatures [12]. The CAVET structure consists of two growth steps, including the first p-i-n substrate growth and the second AlGaN/GaN heterostructure regrowth. During the high-temperature regrowth, Mg dopants from the p-GaN CBL are commonly observed to be heavily incorporated into the subsequent layers, and the formation of 2DEG is hindered by Mg propagation and redistribution to the vicinity of the regrown channel region, resulting in a drastic decrease in the current density level of the device. Lee et al. [13] demonstrated by experiments that the 2DEG completely disappeared when the AlGaN/GaN layers were directly regrown on the Mg-doped p-GaN layer. To circumvent this problem, Chowdhury et al. [14] reported CAVET fabrication using a low-temperature (LT) regrowth by molecular beam epitaxy (MBE) because Mg out-diffusion is readily affected by the growth temperature, and Mg diffusion length is decreased at lower growth temperatures. However, exposing the regrown channel to air during the process causes environmental contaminants at the MBE-regrowth interface, leading to additional difficulties in obtaining good device performance [15]. LT-GaN growth by MOCVD has always been a challenge since the surface quality of GaN is easily degraded using continuous growth at a temperature lower than 900 °C [10]. Agarwal et al. [16] reported MOCVD "pulsed" growth of LT-GaN at a temperature as low as 700 °C with excellent surface morphology and low dislocation density by flow modulation epitaxy (FME) [17], and a sharp drop of the Mg diffusion tail in the subsequent GaN layers was shown in the secondary-ion mass spectrometry (SIMS) profile. Suppression of Mg diffusion was found well through many previous material-centric studies on LT-GaN growth, however, further analysis from the perspective of device fabrication and characterization is needed.

In this work, we focus on the aspect of achieving high on-state current density using an all-MOCVD process, overcoming the various challenges that the device structure presents. It is well known that as the growth temperature is decreasing, the crystal quality of GaN becomes worse with increased defect density. The LT-GaN MSL acts as a sacrificial layer to block Mg propagation, and its material properties also need to be guaranteed that the defect density should not cause leakage problems in the device. Trench CAVETs were designed and fabricated successfully with a LT-GaN Mg stopping layer (MSL) embedded between the p-GaN layer and the AlGaN/GaN heterostructure, which was aimed to block Mg propagation and redistribution. The schematic of the device structure is shown in Figure 1a. The trench CAVET sits on a GaN native substrate to have low dislocation density in the bulk [18]. A MOCVD-grown Mg-doped p-GaN layer serves as the CBL to generate a potential barrier. Selective-area p-type doping is achieved by trench etching to form the aperture region followed by regrowth. The top AlGaN/GaN HEMT structure is regrown by MOCVD to create 2DEG as the source carriers of the trench CAVET. To investigate the influence of MSL regrowth temperature and thickness on the current density level of the device, a total of five trench CAVET samples were fabricated in this experiment with different MSL conditions, as shown in Figure 1b. Three of them had MSL regrown at 750 °C with varying film thicknesses of 10, 50, and 100 nm. The other two samples had MSL regrown at 800 °C with film thicknesses of 10 and 100 nm.

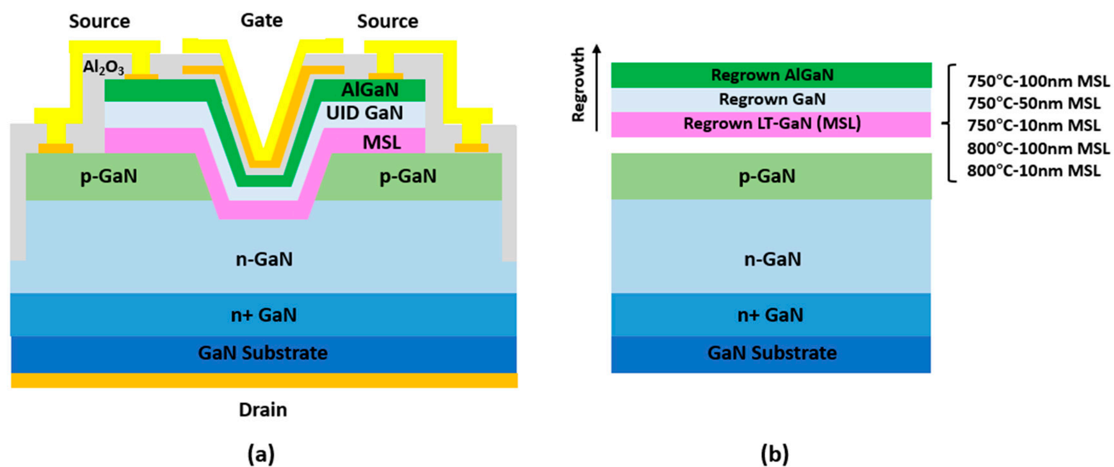

Figure 1. Schematic of (**a**) the GaN trench CAVET used for the device fabrication and (**b**) epitaxial thin film layers with LT-GaN MSLs. LT-GaNs were regrown with different MOCVD growth temperatures and thicknesses.

2. Experimental Procedure

The process flow of the trench-CAVET fabrication is shown in Figure 2. The MOCVD-grown epitaxial structure began with a 2 μm heavily doped n+ GaN layer (Si: ~1×10^{18} cm^{-3}) on a homogeneous GaN substrate, followed by a 1 μm layer of n-type GaN (Si: ~1×10^{17} cm^{-3}) as the drift layer. A 300 nm in-situ p-GaN layer with Mg doping density of 1×10^{19} cm^{-3} was grown on the n-type drift epitaxial layer serving as the CBL. Narrow trenches were etched using Cl_2/BCl_3 gases in inductively coupled plasma-reactive ion etching (ICP-RIE) to create the aperture regions. Tetramethylammonium hydroxide (TMAH) post-treatment was performed after aperture patterning to have a smooth surface of the trench because TMAH provides a much lower etching rate on the $(1\bar{1}00)$ plane of GaN than the other semi-polar planes [19]. After a standard wafer cleaning process, regrowth to fill the trenches was conducted by MOCVD, consisting of a layer of LT-GaN that served as the MSL, a standard high-temperature 140 nm UID-GaN, and a 40 nm $Al_{0.3}Ga_{0.7}N$ grown at 1025 °C, sequentially. Two steps of isolation etching were conducted after the MOCVD regrowth using ICP-RIE for device edge-termination. Then, the Mg dopant in the buried p-GaN layer was activated using rapid thermal annealing (RTA) at 900 °C in nitrogen (N_2) atmosphere because the atomic hydrogen incorporated into the p-GaN during growth forms Mg-H complexes, which requires high-temperature annealing to break the Mg-H bond and diffuse out hydrogen [20]. Subsequently, a multi-layer metal stack consisting of Ti/Al/Ni/Au was deposited on the AlGaN surface as the source contact followed by a RTA annealing process at 800 °C for 45 sec to form an ohmic contact. Ni/Au metal stack on the exposed p-GaN layer formed the p-GaN contact which was later shorted to the source metal through pad connections to avoid CBL punch-through at the off-state and allow fast switching [21]. A 12 nm gate dielectric layer of Al_2O_3 was implemented by atomic layer deposition (ALD), and then Ni/Au gate contact was patterned on top. The Ti/Au unalloyed drain contact was deposited on the backside of the substrate.

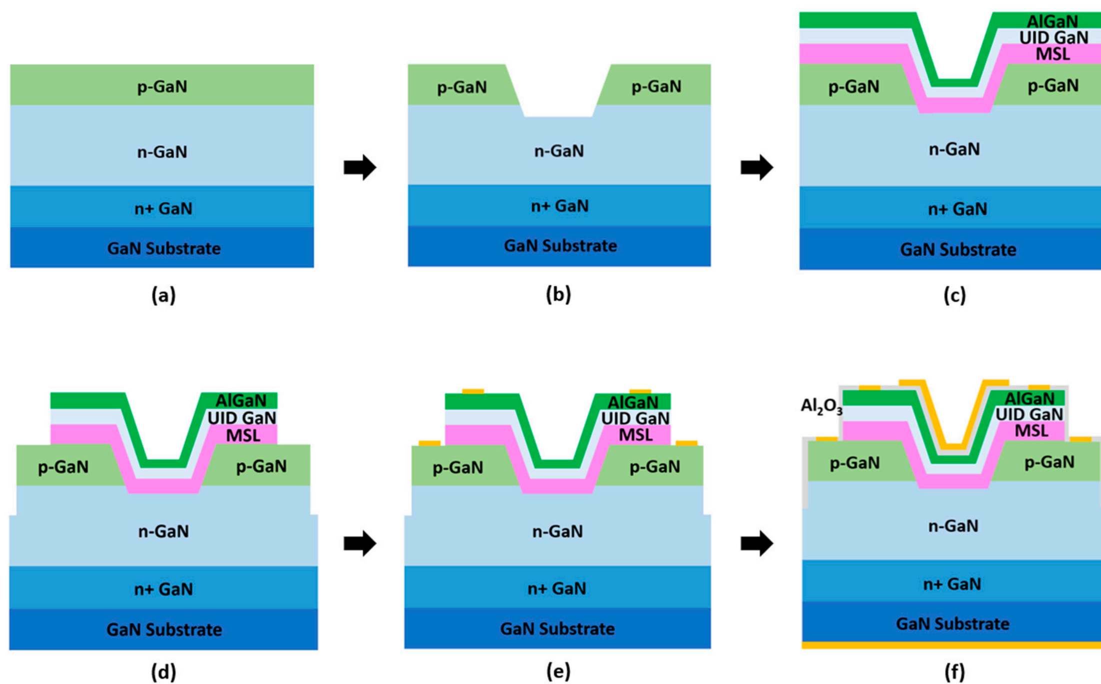

Figure 2. Schematic of the device process flow. (**a**) The p-i-n epitaxial structure containing a 300 nm Mg-doped p-GaN layer on top of a 1-µm n-GaN drift layer. (**b**) Trench etching by ICP-RIE followed by TMAH wet-etching treatment. (**c**) LT-GaN MSL/UID-GaN/AlGaN triple-layer regrowth by MOCVD. (**d**) Two steps of isolation etching by ICP-RIE and Mg dopant activation in the buried p-GaN by RTA in N_2. (**e**) Ti/Al/Ni/Au metal deposition as the source contact followed by source annealing and Ni/Au metal stack as the p-GaN contact connected to the source through pad metallization (not shown in the figure). (**f**) ALD for 12 nm Al_2O_3 as the gate dielectric layer and gate contact formation with Ni/Au. Ti/Au drain contact deposition on the backside.

3. Results and Discussion

To investigate Mg propagation in the MOCVD regrown layers, cross-sections of the partial trench from the five CAVET structures were taken by scanning electron microscopy (SEM), as shown in Figure 3. The schematic of the partial trench region is shown in Figure 3f. The p-GaN region has the highest secondary electron emission intensity and thus appears bright in the SEM image, whereas the n-GaN regions are relatively dark [22]. It can be clearly found from the SEM results that the regrowth thickness in the trench region was not constant, and the trench sidewalls were thicker than the basal plane due to a much faster lateral growth rate by MOCVD. The slope of the p-GaN edge, initially caused by trench etching, showed clear differences among the five trench CAVET structures with different MSL temperatures and thicknesses. Considering the MSL regrowth temperature of 750 °C, 100 nm of MSL prevented Mg out-diffusion most efficiently, presenting the steepest p-GaN slope angle (θ) of 63° and clear p-GaN boundary. θ reduced to 51° for the CAVET with 50 nm MSL and further for 10 nm MSL up to 42°. We believe that the decrease in θ originates from the lateral diffusion of Mg in p-GaN to the regrown aperture region. The top boundary of p-GaN also became more blurred with thinner MSL, which suggested more Mg incorporated into the lateral portion of the channel region above p-GaN. Increasing the regrowth temperature of MSL to 800 °C induced more significant Mg out-diffusion in the CAVETs, as shown in Figure 3d,e. The structure with 100 nm MSL had a further decreased θ of 32°, and the aperture region became much brighter, demonstrating the spread of Mg into the aperture region. For the structure with 10 nm MSL, the white p-GaN region extended to the aperture due to a heavily increased amount of out-diffused Mg, making ambiguous territory between the p-GaN CBL and regrown layers.

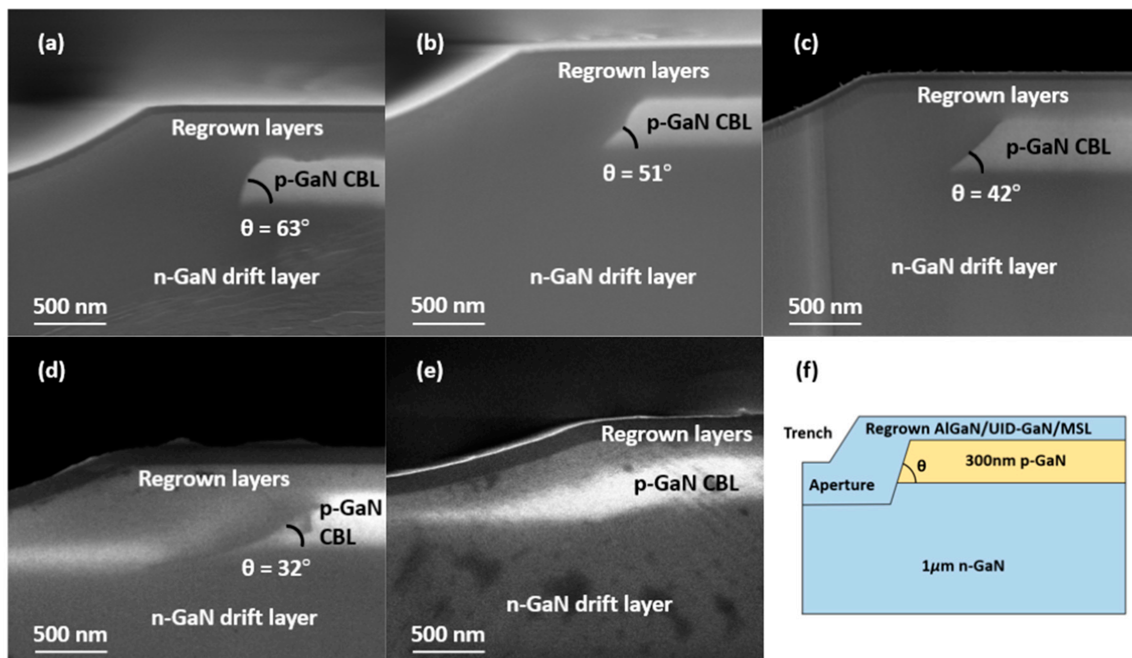

Figure 3. SEM cross-sectional profiles of the partial trench region with (**a**) 100 nm MSL at 750 °C, (**b**) 50 nm MSL at 750 °C, (**c**) 10 nm MSL at 750 °C, (**d**) 100 nm MSL at 800 °C, and (**e**) 10 nm MSL at 800 °C. (**f**) is the schematic of the partial trench region for the SEM images.

The current conductivity of the fabricated trench CAVETs was investigated to understand the impact of MSL thickness and regrowth temperature on the device electrical properties. The I_D-V_{DS} curves of the five CAVETs are shown in Figure 4 a,b. Among the three trench CAVETs with MSL regrown at 750 °C, the devices with 100 nm MSL achieved the highest maximum drain current $I_{D,max}$ of 3.2 kA/cm^2 (drain current density measured at V_{DS} = 7 V, V_{GS} = 0 V) and the lowest specific on-state resistance $R_{on,sp}$ of 1.2 mΩ·cm^2. The trench CAVET with 50 nm MSL showed a decrease in $I_{D,max}$ to 1.5 kA/cm^2 with increased $R_{on,sp}$ of 8.6 mΩ·cm^2, and the device with 10 nm MSL had the lowest $I_{D,max}$ of 800 A/cm^2 and the highest $R_{on,sp}$ of 14.3 mΩ·cm^2. For MSL grown at 800 °C, $I_{D,max}$ of 275 A/cm^2 and $R_{on,sp}$ of 26.4 mΩ·cm^2 were observed for the trench CAVET with 100 nm MSL, and $I_{D,max}$ of 52 A/cm^2 and $R_{on,sp}$ of 70.2 mΩ·cm^2 for the trench CAVET with 10 nm MSL. The I_D-V_{GS} transfer curves of the five devices in Figure 4c exhibit that the threshold voltage V_{TH} of trench CAVET shifts to less negative values with higher MSL temperature and lower MSL thickness. The results reveal that the trench CAVET with MSL regrown at 750 °C retains a much higher current density by more than 10 times compared to the 800 °C-MSL device, and current decrement by higher than 50% happens when the thickness of MSL is halved. From the results, it is believed that the upward diffusion of Mg into the regrown AlGaN/GaN channel suppresses the formation of 2DEG and thus increases the channel resistance, while the lateral diffusion of Mg into the aperture compensates for the n-type dopants and leads to higher aperture resistance. Therefore, both the upward and lateral diffusion of Mg contribute to the significant increase in the total on-resistance of trench CAVET.

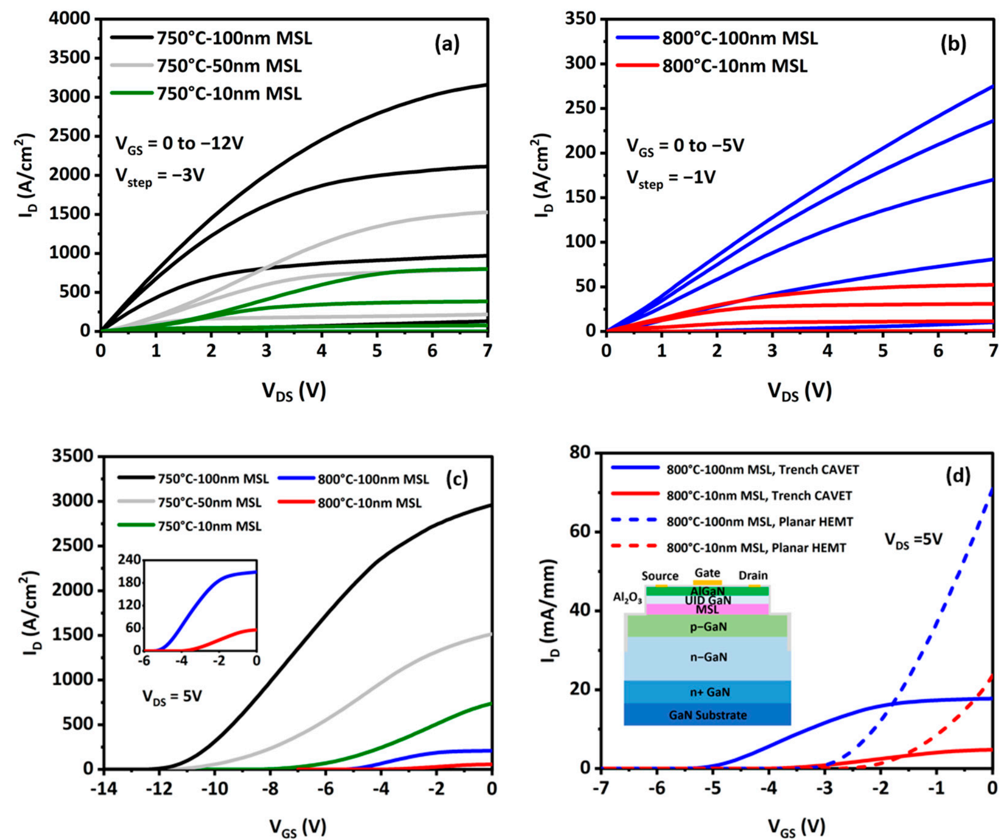

Figure 4. I_D-V_{DS} output characteristics of the fabricated trench CAVETs with varying MSL thicknesses grown at (**a**) 750 °C and (**b**) 800 °C. (**c**) I_D-V_{GS} transfer characteristics of the five fabricated trench CAVETs with different growth thicknesses and temperatures. (**d**) I_D-V_{GS} transfer characteristics comparison between the trench CAVETs and planar HEMTs with MSL grown at 800 °C (the schematic of planar HEMT is shown in the inset).

To further analyze the AlGaN/GaN channel carrier concentration of the trench CAVETs with MSL grown at 800 °C, I_D-V_{GS} transfer curves of the non-trenched CAVET structures as planar HEMTs are compared with trench CAVETs, as shown in Figure 4d. The current unit of the trench CAVETs was transferred to mA/mm for better comparison with the lateral HEMT devices. The on-state drain current level generated by the planar HEMT structure was found to be more than twice that of the trench CAVET for both the cases of 100 nm and 10 nm MSLs. This is because a part of the 2DEG channel of the trench CAVET is located on the semi-polar plane of the slanted trench sidewalls, and thus the total polarization charge is reduced. Nonetheless, the two planar HEMTs show relatively low on-state current density, and it indicates that the 2DEG charge stored at the AlGaN/GaN interface is very limited even for the lateral portion of the regrown channel. Therefore, MSL grown at 800 °C hardly inhibits Mg propagation and leads to a substantial reduction in the channel 2DEG charge, losing the innate advantage of CAVET as a high-current-density device. Increasing the thickness of MSL is beneficial to prevent Mg out-diffusion, but it also increases the distance between the 2DEG channel and the buried p-GaN layer, and thus causes a more negative V_{TH} to deplete the entire thickness of the regrown GaN on top of CBL. From analyzing the I-V measurement results of the five CAVET samples, it is also worth noting that the MSL growth temperature has a more pronounced impact on the on-state current density compared to the film thickness. Therefore, considering the capability of retaining the high current density of a device, we believe that the maximum growth temperature of MSL is lower than 800 °C. However, previous studies have shown that the crystal properties of the regrown GaN layers deteriorate significantly when the MOCVD growth temperature is too low (<700 °C) [16], which may lead to device leakage problems.

The fabricated trench CAVET with a 100 nm MSL regrown at 750 °C achieved the best device performance among the five samples. Figure 5a shows the I_D-V_{DS} output characteristics of the device with gate voltage swept from 0 V to −11 V in steps of −1 V. The double-swept I_D-V_{GS} transfer characteristics of the device shown in Figure 5b exhibit V_{TH} of −11 V and on-off ratio (I_{on}/I_{off}) of 10^6. Thanks to the high quality of the ALD Al_2O_3 gate dielectric layer, the gate leakage current density I_G is about two orders of magnitude lower than the off-state drain current density, and the clockwise hysteresis value of I_D is only 0.1 V. The off-state characteristics of the device in Figure 5c show that the measured three-terminal breakdown voltage of the trench CAVET is 50 V sustained by a 1 μm thick drift layer with n-type doping density of ~10^{17} cm^{-3} by design. A thicker epitaxial drift layer with less n-type doping density can be adopted in the future to improve the breakdown voltage of the device. Additionally, the breakdown voltage of the source-to-drain n-p-n body diode was measured by applying a positive bias on the bottom electrode and ground on top, as plotted in Figure 5d, to illustrate the blocking capability of the p-GaN CBL. A two-terminal breakdown voltage of 180 V was achieved successfully, suggesting that the buried p-GaN CBL was effectively activated by RTA with an estimated peak electric field of 3.6 MV/cm.

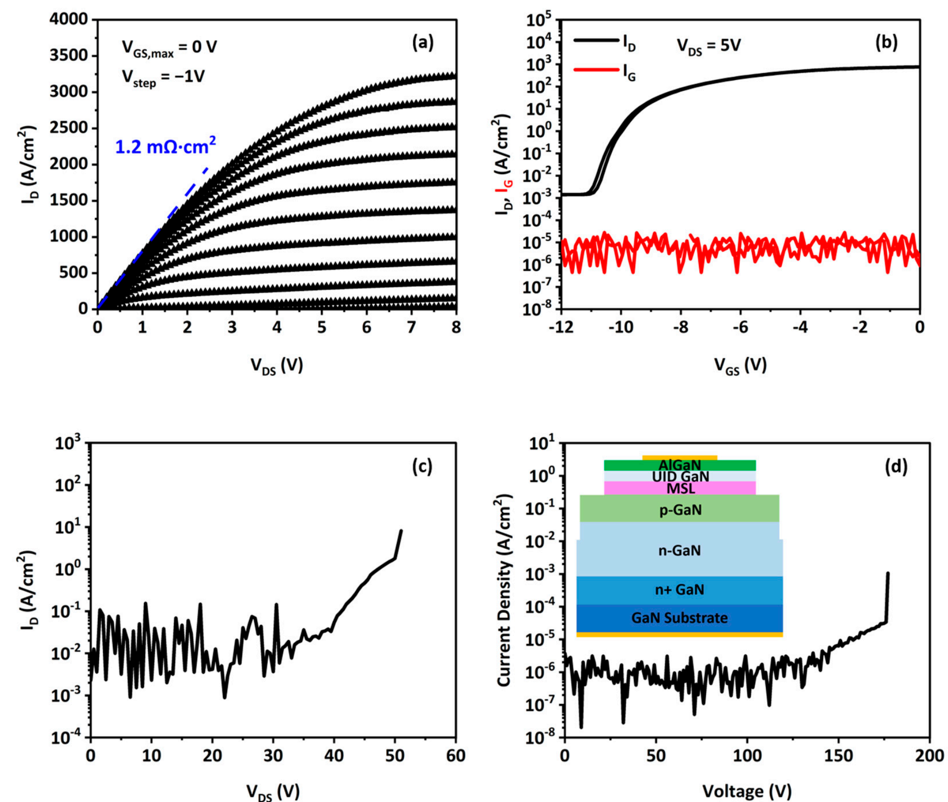

Figure 5. (**a**) I_D-V_{DS} output characteristics, (**b**) I_D-V_{GS} transfer characteristics, and (**c**) off-state characteristics of the fabricated trench CAVET inserted with a 100 nm MSL grown at 750 °C. (**d**) Two-terminal reverse breakdown characteristics of the source-to-drain n-p-n body diode (the schematic of the test structure is shown in the inset).

In Figure 6, the reverse leakage current was measured from the regrown p-n junction for electrical characteristics of the regrown LT-GaN at 750 °C. The test structure shown in Figure 6a has similar epitaxial layers of CAVET except for the regrown n+ GaN (Si: ~5×10^{18} cm^{-3}) replacing the AlGaN layer. A low reverse leakage current of the isolated regrown p-n junction is displayed in Figure 6b, which reflects that the quality of the regrown layers as well as the interface is suited for device fabrication. The atomic force microscopic (AFM) image of the regrown LT-GaN at 750 °C is shown in Figure 6c with a root mean square (RMS) surface roughness of 2.48 nm. As a sacrificial layer, the 750 °C regrown LT-

GaN effectively suppresses Mg out-diffusion and supports high current conductivity of the AlGaN/GaN heterostructure without causing severe leakage issues for device performance.

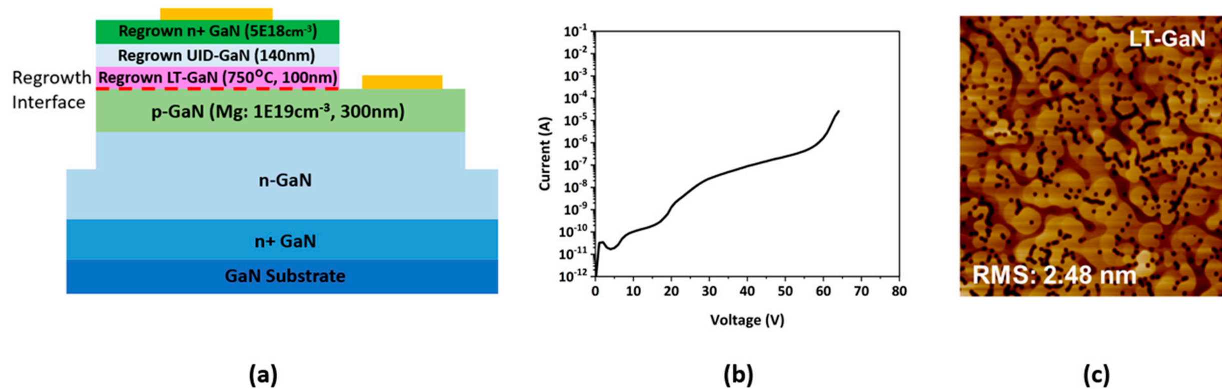

Figure 6. Characteristics of the MOCVD regrown LT-GaN at 750 °C. (**a**) The schematic of isolated regrown p-n test structure. (**b**) Reverse leakage current measured from the test structure in (**a**). (**c**) AFM image of the regrown LT-GaN at 750 °C.

Figure 7 shows the SIMS depth profiles of four test samples with the same epitaxial layers as CAVET, three of which contained a 100 nm ex situ regrown LT-GaN layer at different temperatures (750 °C, 800 °C, and 850 °C, respectively), and a reference sample whose ex-situ regrown layer was a 100 nm high-temperature UID-GaN grown at 1025 °C, the standard temperature for GaN channel regrowth. The vertical dotted line in the figure represents a borderline to distinguish Mg residual tails in the regrown layers from Mg plateau in p-GaN CBL. The calculated decay rate of Mg tail in the UID-GaN layer regrown at 1025 °C was ~104 nm/decade, and it was decreased to ~64 nm/decade in the 850 °C-MSL, ~53 nm/decade in the 800 °C-MSL, and ~39 nm/decade in the 750 °C-MSL. Compared to high-temperature GaN regrowth at 1025 °C, the 750 °C-MSL effectively reduced the Mg diffusion decay rate by 62.5%. A narrow Mg spike was also found at the regrowth interface, and the gettering of Mg was likely due to the high defect density of the regrowth interface [12]. Comparing the SIMS profiles at the regrowth interface of the four samples with different first regrown layers (1025 °C-, 850 °C-, 800 °C-, and 750 °C-GaN), the spike level was slightly increased with decreasing regrowth temperature, implying that a decrease in regrowth temperature may induce higher defect density at the growth interface.

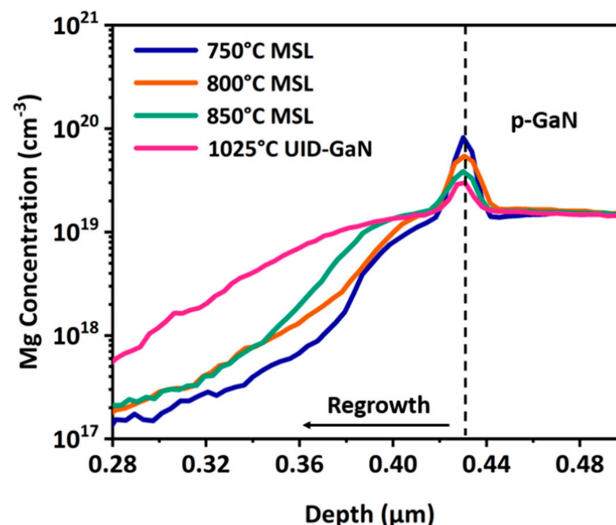

Figure 7. SIMS depth profiles of Mg in four test samples with different regrowth temperatures on p-GaN.

4. Conclusions

The out-diffusion of Mg from the p-GaN CBL into the regrown AlGaN/GaN layers was always a challenge in preventing CAVETs from generating high current density in power electronic applications. Insertion of a MOCVD-regrown LT-GaN layer as MSL to overcome Mg propagation was investigated in this letter by comparing five fabricated trench CAVET samples with different growth temperatures and thicknesses of MSL. An efficient MSL growth recipe, 100 nm LT-GaN grown at 750 °C, was obtained in inhibiting Mg propagation and retaining high current conductivity, and the corresponding CAVET device inserting this layer achieved high current density of 3.2 kA/cm^2 and low $R_{on,sp}$ of 1.2 mΩ·cm^2. The buried p-n body junction of the device sustained a two-terminal breakdown voltage of 180 V, showing an estimated peak electric field of 3.6 MV/cm. The SIMS depth profiles of Mg in the regrown GaN layer demonstrated that, compared with high-temperature MOCVD regrowth at 1025 °C, the 750 °C-MSL significantly decreased the Mg diffusion decay rate from ~104 nm/decade to only ~39 nm/decade. We reported the use of LT-GaN MSL for achieving high-current-density trench CAVET using an all-MOCVD process from a device perspective for the first time. This work provides valuable insights into the development of high-current-density CAVET switching transistors for future power electronics applications.

Author Contributions: X.W. was responsible for device design, fabrication, data analysis and the writing of the manuscript. K.J.L. was responsible for epitaxial design and the MOCVD growth. X.W. and Y.N. were responsible for electrical measurements. X.W. and J.C. were responsible for the device process design. S.C. was responsible for conceiving the idea and the overall project supervision. K.J.L., Y.N., J.C. and S.C. were responsible for the manuscript review and editing. All authors have read and agreed to the published version of the manuscript.

Funding: This research was funded by the KYOCERA Corporation, Japan.

Data Availability Statement: Not applicable.

Acknowledgments: The experimental work was performed in Stanford Nanofabrication Facility (SNF) and Stanford Nano Shared Facilities (SNSF).

Conflicts of Interest: The authors declare no conflict of interest.

References

1. Jones, E.A.; Wang, F.F.; Costinett, D. Review of Commercial GaN Power Devices and GaN-Based Converter Design Challenges. *IEEE J. Emerg. Sel. Top. Power Electron.* **2016**, *4*, 707–719. [CrossRef]
2. Chu, R. GaN power switches on the rise: Demonstrated benefits and unrealized potentials. *Appl. Phys. Lett.* **2020**, *116*, 090502. [CrossRef]
3. Nie, H.; Diduck, Q.; Alvarez, B.; Edwards, A.P.; Kayes, B.M.; Zhang, M.; Ye, G.; Prunty, T.; Bour, D.; Kizilyalli, I.C. 1.5-kV and 2.2-mΩ·cm^2 Vertical GaN Transistors on Bulk-GaN Substrates. *IEEE Electron Device Lett.* **2014**, *35*, 939–941. [CrossRef]
4. Kachi, T. State-of-the-art GaN vertical power devices. In Proceedings of the 2015 IEEE International Electron Devices Meeting (IEDM), Washington, DC, USA, 7–9 December 2015; pp. 16.11.11–16.11.14.
5. Yeluri, R.; Lu, J.; Hurni, C.A.; Browne, D.A.; Chowdhury, S.; Keller, S.; Speck, J.S.; Mishra, U.K. Design, fabrication, and performance analysis of GaN vertical electron transistors with a buried p/n junction. *Appl. Phys. Lett.* **2015**, *106*, 183502. [CrossRef]
6. Ji, D.; Gupta, C.; Chan, S.H.; Agarwal, A.; Li, W.; Keller, S.; Mishra, U.K.; Chowdhury, S. Demonstrating >1.4 kV OG-FET performance with a novel double field-plated geometry and the successful scaling of large-area devices. In Proceedings of the 2017 IEEE International Electron Devices Meeting (IEDM), San Francisco, CA, USA, 2–6 December 2017; pp. 9.4.1–9.4.4.
7. Li, W.; Ji, D.; Tanaka, R.; Mandal, S.; Laurent, M.; Chowdhury, S. Demonstration of GaN static induction transistor (SIT) using self-aligned process. *IEEE J. Electron Devices Soc.* **2017**, *5*, 485–490. [CrossRef]
8. Ji, D.; Agarwal, A.; Li, H.; Li, W.; Keller, S.; Chowdhury, S. 880 V/2.7 mΩ·cm^2 MIS Gate Trench CAVET on Bulk GaN Substrates. *IEEE Electron Device Lett.* **2018**, *39*, 863–865. [CrossRef]
9. Shibata, D.; Kajitani, R.; Ogawa, M.; Tanaka, K.; Tamura, S.; Hatsuda, T.; Ishida, M.; Ueda, T. 1.7 kV/1.0 mΩ·cm^2 normally-off vertical GaN transistor on GaN substrate with regrown p-GaN/AlGaN/GaN semipolar gate structure. In Proceedings of the 2016 IEEE international electron devices meeting (IEDM), San Francisco, CA, USA, 3–7 December 2016; pp. 10.11.11–10.11.14.
10. Mandal, S.; Agarwal, A.; Ahmadi, E.; Bhat, K.M.; Ji, D.; Laurent, M.A.; Keller, S.; Chowdhury, S. Dispersion free 450-V p GaN-gated CAVETs with Mg-ion implanted blocking layer. *IEEE Electron Device Lett.* **2017**, *38*, 933–936. [CrossRef]

11. Ji, D.; Laurent, M.A.; Agarwal, A.; Li, W.; Mandal, S.; Keller, S.; Chowdhury, S. Normally OFF trench CAVET with active Mg-doped GaN as current blocking layer. *IEEE Trans. Electron Devices* **2016**, *64*, 805–808. [CrossRef]
12. Xing, H.; Green, D.S.; Yu, H.; Mates, T.; Kozodoy, P.; Keller, S.; DenBaars, S.P.; Mishra, U.K. Memory Effect and Redistribution of Mg into Sequentially Regrown GaN Layer by Metalorganic Chemical Vapor Deposition. *Jpn. J. Appl. Phys.* **2003**, *42*, 50–53. [CrossRef]
13. Lee, K.J.; Nakazato, Y.; Chun, J.; Wen, X.; Meng, C.; Soman, R.; Noshin, M.; Chowdhury, S. Nanoporous GaN on p-type GaN: A Mg out-diffusion compensation layer for heavily Mg-doped p-type GaN. *Nanotechnology* **2022**, *33*, 505704. [CrossRef] [PubMed]
14. Chowdhury, S.; Wong, M.H.; Swenson, B.L.; Mishra, U.K. CAVET on Bulk GaN Substrates Achieved With MBE-Regrown AlGaN/GaN Layers to Suppress Dispersion. *IEEE Electron Device Lett.* **2012**, *33*, 41–43. [CrossRef]
15. Ji, D.; Agarwal, A.; Li, W.; Keller, S.; Chowdhury, S. Demonstration of GaN Current Aperture Vertical Electron Transistors With Aperture Region Formed by Ion Implantation. *IEEE Trans. Electron Devices* **2018**, *65*, 483–487. [CrossRef]
16. Agarwal, A.; Tahhan, M.; Mates, T.; Keller, S.; Mishra, U. Suppression of Mg propagation into subsequent layers grown by MOCVD. *J. Appl. Phys.* **2017**, *121*, 025106. [CrossRef]
17. Kobayashi, N.; Makimoto, T.; Horikoshi, Y. Flow-Rate Modulation Epitaxy of GaAs. *Jpn. J. Appl. Phys.* **1985**, *24*, L962. [CrossRef]
18. You, S.; Geens, K.; Borga, M.; Liang, H.; Hahn, H.; Fahle, D.; Heuken, M.; Mukherjee, K.; De Santi, C.; Meneghini, M.; et al. Vertical GaN devices: Process and reliability. *Microelectron. Reliab.* **2021**, *126*, 114218. [CrossRef]
19. Kodama, M.; Sugimoto, M.; Hayashi, E.; Soejima, N.; Ishiguro, O.; Kanechika, M.; Itoh, K.; Ueda, H.; Uesugi, T.; Kachi, T. GaN-Based Trench Gate Metal Oxide Semiconductor Field-Effect Transistor Fabricated with Novel Wet Etching. *Appl. Phys. Express* **2008**, *1*, 021104. [CrossRef]
20. Li, W.; Nomoto, K.; Lee, K.; Islam, S.; Hu, Z.; Zhu, M.; Gao, X.; Xie, J.; Pilla, M.; Jena, D. Activation of buried p-GaN in MOCVD-regrown vertical structures. *Appl. Phys. Lett.* **2018**, *113*, 062105. [CrossRef]
21. Döring, P.M. Experimental Evaluation of the Device Design and Process Technology of the Current Aperture Vertical Electron Transistor for Power Electronics Applications. Ph.D. Thesis, Universität Freiburg, Freiburg im Breisgau, Germany, 2021.
22. Alugubelli, S.R.; Fu, H.; Fu, K.; Liu, H.; Zhao, Y.; Ponce, F.A. Dopant profiling in pin GaN structures using secondary electrons. *J. Appl. Phys.* **2019**, *126*, 015704. [CrossRef]

Disclaimer/Publisher's Note: The statements, opinions and data contained in all publications are solely those of the individual author(s) and contributor(s) and not of MDPI and/or the editor(s). MDPI and/or the editor(s) disclaim responsibility for any injury to people or property resulting from any ideas, methods, instructions or products referred to in the content.